

Flocculation model of cohesive sediment using variable fractal dimension

Minwoo Son · Tian-Jian Hsu

Received: 28 August 2007 / Accepted: 17 December 2007 / Published online: 5 January 2008
© Springer Science+Business Media B.V. 2008

Abstract A new flocculation model using variable fractal dimension is proposed and validated with several experimental data and an existing model. The proposed model consists of two processes: aggregation and breakup due to flow turbulence. For aggregation process, the aggregate structure is considered to have the characteristic of self-similarity, the main concept of fractal theory. Under this assumption, a variable fractal dimension instead of a fixed one adopted by previous studies is utilized here for general cohesive sediment transport. For breakup, similar concept is adopted in a more empirical manner because breakup is too abrupt to entirely apply the concept of variable fractal dimension. By a linear combination of the formulations for aggregation and breakup processes, a flocculation model which can describe the temporal evolution of floc size is obtained. Flocculation model using variable fractal dimension is capable of predicting equilibrium floc size when compared with several experimental data sets using different types of mud provided that empirical coefficients are calibrated. Through model-data comparison with Manning and Dyer (Marine Geology 160:147–170, 1999), it is also clear that some of the empirical coefficients may depend on sediment concentration. Model results for the temporal evolution of floc size are less satisfactory, despite model results shows a more smooth “S-curve” for the temporal evolution of floc size as compared with the previous model using fixed fractal dimension. The proposed model is limited to mono-size of primary particle and dilute flow condition. These other features shall be investigated as future work.

Keywords Flocculation · Cohesive sediment · Aggregation · Breakup · Fractal dimension · Equilibrium floc size

M. Son (✉) · T.-J. Hsu
Department of Civil and Coastal Engineering, University of Florida, 365 Weil Hall, P.O. Box 116580,
Gainesville, FL 32611-6580, USA
e-mail: sonmw@ufl.edu

T.-J. Hsu
e-mail: thsu@ufl.edu

Abbreviations

n	Number of flocs per unit volume
D, d	Size of floc and primary particle
D_e	Equilibrium floc size
G	Dissipation parameter (shear rate)
ε	Dissipation rate of energy
ν	Kinematic viscosity
t	Time
e_b, e_c, e_d	Efficiency parameter
ϕ	Volumetric concentration
c	Mass concentration
ρ_s, ρ_f, ρ_w	Density of primary particle, floc, and water
f_s	Shape factor
F	Three-dimensional fractal dimension of floc
α, β, a, p, q	Coefficient
F_c	Characteristic fractal dimension
D_{fc}	Characteristic size of floc
μ	Dynamic viscosity of the fluid
F_y	Yield strength of floc
λ_0	Kolmogorov micro scale,
k'_A, k'_B	Empirical dimensionless coefficient
X	Ratio of the equilibrium floc size to primary particle size
F_n	Function

1 Introduction

Water movement in natural environment, such as river, estuary and coastal zone often carries sediment particles of various properties. Sediment transport is one of the most important processes that have to be understood in order to further predict the morphological evolution and the carrier flow hydrodynamics (e.g., bottom friction). In a broad sense, sediment can be classified into non-cohesive sediment and cohesive sediment. Non-cohesive sediments are in general of coarser grain size, such as sand and gravel. Their electrochemical or biochemical attraction is not sufficient to aggregate particles and as a result, particles move individually. Cohesive sediments are the mixture of fine-grained sediment, such as clay particles, silt, fine sand, organic material and so on. These sediments possess cohesive characteristics because of the electrochemical attraction of clay particles and organic material [50]. Fine-grained sediments in rivers, estuaries and coastal waters form aggregated particles (or flocs) through binding together of primary particles, and flocs can disaggregate into smaller flocs/particles through flow shear or collisions. This is the flocculation process [8]. Floc dynamics depends on flow condition, and physical and biological–chemical properties of water and primary particles. The evolution of floc size and effective density directly determines the settling velocity which is one of the most fundamental quantities that must be specified in order to calculate sediment transport [29,43].

The flocculation process has been studied by many researchers. The theoretical aspects of the flocculation process have been developed by pioneering studies such as Smoluchowski [35], Camp and Stein [7], and Ives [15]. These studies have been based on the rate of change of particle numbers due to particle aggregation after collision [41]. Lick and Lick [23] present a more general model for floc dynamics that includes the effects of disaggregation due to

collision and shear. Tsai et al. [42] investigate the effect of fluid shear with natural bottom sediments and suggest the important factors of collision mechanism according to particle sizes. Lick et al. [22] further study the effect of differential settling on flocculation of fine-grained sediments using natural sediments. McAnally and Mehta [26] develop a dynamical formulation for estuarine fine sediment aggregation. The spectrum of fine particle has been represented by a discrete number of classes and the frequency of particle collisions due to Brownian motion, turbulent shearing and differential settling are described by statistical relationships. They conclude that it is vary important to characterize particle density and strength when flocculation approaches equilibrium state.

The flocculation of fine-grained particles depends on collisions resulted from Brownian motion, differential settling, and fluid shear due to flow turbulence [8,9,22]. According to the studies of O'Melia [33], McCave [27], Van Leussen [44], and Stolzenbach and Elimelech [36], it can be concluded that for cohesive sediment transport in estuaries and continental shelves (or other aquatic system with more energetic flow) the effects of Brownian motion and differential settling on the flocculation process may be less important. Hence, many studies have focused on understanding the effects of turbulence on the flocculation process. Parker et al. [34] describe the change of number of particles in a turbulent flow as a function of G , the dissipation parameter (or shear rate) defined as $\sqrt{\varepsilon/\nu}$. Herein, ε is the turbulent dissipation rate and ν is the kinematic viscosity of the fluid. It is important to note that G is a measure of the small scale turbulent shear. To control G , many studies use a mixing tank. Ayesa et al. [3] develop an algorithm to calibrate the parameters proposed by Argamam and Kaufman [2] using data obtained from mixing tank experiments. Tambo and Hozumi [37] conclude that the maxima floc size is in proportional to the Kolmogorov turbulent length scale. However, none of these studies explicitly describes the variation of floc size with time, which may be necessary for a proper understanding and modeling of the sediment transport processes in dynamical environment, especially wave-dominated condition [13,14,40,48].

Biggs and Lant [4] conduct experiments in order to obtain the temporal change of floc size with respect to a prescribed constant dissipation rate. In this experiment, samples of activated sludge are stirred in a batch mixing vessel. They conclude that the change in floc size with flow shear follows a power law relationship due to the breakage mechanisms. Bouyer et al. [5] analyze the relationship between characteristic floc size and turbulent flow characteristics in a mixing tank. This experiment demonstrates that the average floc sizes are similar after flocculation or reflocculation steps, but the floc size distributions can be different with different impellers. Manning and Dyer [24] investigate the relationship between floc size and dissipation parameter under different sediment concentrations using an annular flume. They conclude that at low shear rate, increasing turbidity encourages floc growth. However, at high shear rate, increasing turbidity in suspension may enhance breakup of floc.

Winterwerp [47,48] develops a flocculation model adopting fractal theory. The concept of fractal geometry has been used widely in order to describe floc geometry (see [19,45] for a review). Winterwerps's model describes one characteristic floc size and considers turbulence as the dominant factor affecting flocculation processes. However, a fixed value of fractal dimension such as 2.0 and 2.2 [47,49] has been assumed in the model. Although it is practical and for the sake of simplicity to use a fixed fractal dimension, the applicability of this assumption for sediment transport in different regimes is questionable. For example, fractal dimension of floc in the water column of dilute flow is considered to be around 2.0 [11,28]. However, noticeable variations of fractal dimension are obtained based on field observed estuaries mud [9]. Moreover, using measured data and constitutive relations for rheology [19], effective stress and permeability [30] in a consolidating bed, the resulting fractal dimension

is significantly larger than 2.0 (around 2.75). As illustrated by Khelifa and Hill [17], conceptually in a completely consolidated bed, where all the floc structure is completely destroyed, the fractal dimension is 3.0. Hence, a general flocculation model that is able to describe floc dynamics from consolidating bed to dilute suspension must incorporate variable fractal dimension.

Khelifa and Hill [17] propose a model to predict the effective density of flocs and the resulting settling velocity using a variable fractal dimension that depends on floc size. They demonstrated that by using the concept of variable fractal dimension, the resulting settling velocity converges to Stokes' law when the floc size approaches to that of the primary particle. On the other hand, as the floc size becomes very large (more than about 2 mm), the settling velocity decreases as floc size increases. Consequently, Khelifa and Hill [17] suggest a new settling velocity formulation that is able to predict measured settling velocity data reported previously for a much wider range of floc sizes. In this study, we continue the work of Khelifa and Hill [17]. We apply the variable fractal dimension concept of Khelifa and Hill [17] to the floc dynamics formulation suggested by Winterwerp [47] to predict the temporal evolution of floc size.

It is important to extend the concept of variable fractal dimension to calculate the floc dynamics. Recently, numerical models for fine sediment transport have become popular. These numerical models are capable of calculating averaged fluid flow, turbulence and sediment concentration in the water column [10,43,46], fluid mud transport near the bed [14,48] as well as sedimentation and consolidation processes [31,39]. However, the floc dynamic in most of these models are not explicitly considered. What are needed in these numerical models are additional governing equations for floc sizes, such as that proposed by Winterwerp [47] or Hill and Newell [12] that can be coupled with the hydrodynamic and sediment transport calculations. Hence, the main objective of this paper is to extend the flocculation model of Winterwerp [47] for variable fractal dimension [17] in dilute flow condition.

This paper is organized as follows. We first present a formulation of floc size evolution integrated with fractal theory (Sect. 2). In Sect. 3, model results for equilibrium floc size and time evolution of floc size are compared with measured data in the mixing tank [4,5] and annular flume [24] as well as earlier model results based on fixed fractal dimension [47]. This paper is concluded in Sect. 4 with a note on the future work.

2 Flocculation model using variable fractal dimension

2.1 Aggregation processes

When modeling cohesive sediment transport, the change of floc size needs to be considered because the settling velocity depends on floc size. On the other hand, the carrier flow turbulence can be damped due to the presence of sediment. This mechanism may directly or indirectly depend on floc size [14,47]. Thus, it is important to develop a model simulating the temporal evolution of floc size under given flow conditions. The main concept of fractal theory is self-similarity of the floc structure. Under this assumption, the concept of fractal theory can be used to develop a model describing the floc aggregation process. The model development adopted in this paper is based on previous two studies of Winterwerp [47] for floc dynamics and Khelifa and Hill [17] for variable fractal dimension.

Levich [21] proposes the rate of coagulation between the particles in a turbulent fluid:

$$\frac{dn}{dt} = -\frac{3}{2}e_c\pi e_dGD^3n^2 \tag{1}$$

where n is the number of flocs per unit volume, D is floc size, t is time, e_c is an efficiency parameter accounting for the fact that not all encounters result in coagulation, and e_d is another efficiency parameter for diffusion: see Winterwerp [47] and Van Leussen [44] for more details.

For cohesive sediment, the volumetric concentration, ϕ , can be expressed by mass concentration, c , and the number of flocs per unit volume, n [47].

$$\phi = \left(\frac{\rho_s - \rho_w}{\rho_f - \rho_w}\right) \frac{c}{\rho_s} = f_s n D^3 \tag{2}$$

where ρ_s is the density of primary particle, ρ_f is the density of floc, ρ_w is the water density, and f_s is a shape factor taken to be $\pi/6$ for spherical particles.

For monosized primary particles of size d , the effective density of floc is calculated as [19]:

$$\rho_f - \rho_w = (\rho_s - \rho_w) \left(\frac{D}{d}\right)^{F-3} \tag{3}$$

where F is the three-dimensional fractal dimension of flocs. To take into account the possible variability in the structure of flocs, a variable fractal dimension depending on floc size is proposed by Khelifa and Hill [17]. The fractal dimension of a floc with size closer to the size of the primary particles should approach the value of 3.0 [17]. On the other hand, the fractal dimension of large flocs should be close to the value of 2.0 [8,9,28,47]. Hence, a power law is proposed by Khelifa and Hill [17] to describe variation of fractal dimension:

$$F = \alpha \left(\frac{D}{d}\right)^\beta \tag{4}$$

where $\alpha = 3$ and $\beta = \frac{\log(F_c/3)}{\log(D_{fc}/d)}$. F_c is a characteristic fractal dimension and D_{fc} is a characteristic size of flocs. Khelifa and Hill [17] suggest the typical value of F_c and D_{fc} to be $F_c = 2.0$ and $D_{fc} = 2,000 \mu\text{m}$. Equation 4 gives a plausible description of fractal dimension such that when $d \ll D$, F approaches 3.0 but for very large floc, F approaches 2.0.

By combining Eqs. 2 and 3, n can be represented as:

$$n = \frac{c}{\rho_s f_s} d^{F-3} D^{-F} \tag{5}$$

and $\frac{dn}{dD}$ can be calculated as:

$$\frac{dn}{dD} = -\frac{3c}{\rho_s f_s} d^{F-3-\beta} D^{-F-1+\beta} \left(\beta \ln \frac{D}{d} + 1\right) \tag{6}$$

Utilizing $\frac{dD}{dt} = \frac{dD}{dn} \frac{dn}{dt}$ and Eqs. 1 and 6, we obtain an equation representing the evolution of floc size due to aggregation:

$$\frac{dD}{dt} = \frac{ce_c\pi e_d}{2\rho_s f_s} G d^{F-3+\beta} D^{-F+4-\beta} \frac{1}{\beta \ln \frac{D}{d} + 1} \tag{7}$$

2.2 Breakup process

As mentioned previously, the concept of fractal theory is based on self-similarity of the structure. Although this is appropriate for aggregation process, breakup process may be too abrupt to entirely adopt variable fractal dimension. Following Winterwerp [17], we assume inter-particle collisions are apt to cause aggregation of flocs rather than breakup. Hence, only the breakup by turbulent shear stress is incorporated here. Winterwerp [17] suggests that the breakup rate is a function of the dissipation parameter, G , of the disrupting turbulent eddies and proposes the following relation based on dimensional considerations:

$$\frac{1}{n} \frac{dn}{dt} \propto Ga \left(\frac{D-d}{d} \right)^p \left(\frac{\mu G}{F_y/D^2} \right)^q \quad (8)$$

where μ is the dynamic viscosity of the fluid, F_y is the yield strength of flocs, and a , p , and q are the coefficients to be discussed later. By further incorporating an efficiency parameter for floc breakup, e_b , Eq. 8 can be written as:

$$\frac{dn}{dt} = ne_b Ga \left(\frac{D-d}{d} \right)^p \left(\frac{\mu G}{F_y/D^2} \right)^q \quad (9)$$

Substituting Eqs. 5 and 6 into Eq. 9, the balance equation for the decay rate of flocs by breakup process can be written as:

$$\frac{dD}{dt} = -\frac{e_b Ga}{3} \left(\frac{\mu G}{F_y} \right)^q d^{\beta-p} D^{-\beta+1+2q} (D-d)^p \frac{1}{\beta \ln \frac{D}{d} + 1} \quad (10)$$

Although p and q are essentially empirical coefficients, their (approximate) values can be estimated based on some physical considerations. Many experimental studies suggest that floc size is proportional to the Kolmogorov length scale [1,6,20], $\lambda_0 (= (\nu^3/\varepsilon)^{1/4})$, where ν is the kinematic viscosity of fluid and ε is the turbulent dissipation rate. Hence, Winterwerp [47] assumes that the equilibrium floc size, D_e , is in proportion to $1/\sqrt{G}$. Further assuming that the equilibrium floc size is much larger than primary particle size, Winterwerp [47] suggests $p = 1.0$ and $q = 0.5$ in his flocculation model using fixed fractal dimension. In the present study using variable fractal dimension, it is necessary to check the robustness and the sensitivity of p and q in the context of variable fractal dimension. This issue shall be discussed in the next section.

2.3 Flocculation model

Using a linear combination of aggregation and breakup processes [47], i.e., Eqs. 7 and 10, a complete flocculation model can be obtained:

$$\frac{dD}{dt} = \frac{Gd^\beta}{\beta \ln \frac{D}{d} + 1} \left[\frac{ce_c\pi e_d}{2\rho_s f_s} d^{F-3} D^{-F+4-\beta} - \frac{e_b a}{3} \left(\frac{\mu G}{F_y} \right)^q d^{-p} D^{-\beta+2q+1} (D-d)^p \right] \quad (11)$$

where $k'_A = \frac{3e_c\pi e_d}{2f_s}$ and $k'_B = ae_b$ are empirical dimensionless coefficients.

For equilibrium condition, i.e., $dD/dt = 0$, and using the assumption that D_e is much larger than d , Eq. 11 can be simplified as:

$$F_n(X) = (X)^{3X^\beta + (p+2q-3)} - \frac{c}{\rho_s} \frac{k'_A}{k'_B} \left(\frac{\mu G d^2}{F_y} \right)^{-q} = 0 \quad (12)$$

where $X = D_e/d$. Equation 12 is a nonlinear algebraic equation of D_e . Numerical solution for equilibrium floc size can be obtained by setting F_n zero. In this study, we will directly calculate numerical solution of the time evolution equation of floc size, i.e., Eq. 11, using a Runge-Kutta method. However, it is important to first examine the effects of p and q on the flocculation model using Eq. 12 because their behavior affects the nonlinearity and hence numerical stability of time evolution Eq. 11. Figure 1a shows the variation of $F_n(X)$ with X for three flocculation experiments: T69, T71, and T73 carried out in Delft Hydraulics (see [44]). Flow conditions and coefficients are shown in Table 1. Using values suggested by Winterwerp [47], $p = 1.0$, $q = 0.5$ (and with $k'_A = 0.15$ and $k'_B = 10^{-5}$), Eq. 12 has solution (i.e., for the range $X > 1$, $F_n(X) = 0$ exist). Figure 1b further presents the evolution of $F_n(X)$ with several p values for test T71 but with q remains 0.5. When p is as large as 1.3, $F_n(X)$ approaches zero rapidly and the resulting D_e is very close to d (i.e., $D_e/d = 3.15$). Moreover, when setting p to be 0.7, $F_n(X)$ has no root and the equilibrium floc size does not exist. That is, Eq. 12 and the flocculation model, Eq. 11, become unrealistic when $p = 0.7$. Figure 1c further shows the evolution of $F_n(X)$ with several q values for test T71 with $p = 1.0$. When q is 0.7, $F_n(X)$ increases rapidly with respect to X . In contrast, $F_n(X)$ increases very slowly when q is 0.3. Hence, when q is smaller than 0.3, a highly accurate and stable numerical solver is necessary in order to obtain a solution for Eq. 11. From these observations, it can be concluded that values of $p = 1.0$ and $q = 0.5$ originally suggested by Winterwerp [47] based on physical arguments are also rather robust numerically for the present flocculation model using variable fractal dimension.

When the values suggested by Winterwerp [47] for $p = 1.0$ and $q = 0.5$ are adopted for the present model using variable fractal dimension, Eq. 11 can be rewritten as:

$$\frac{dD}{dt} = \frac{Gd^\beta}{\beta \ln \frac{D}{d} + 1} \left[\frac{c}{3\rho_s} k'_A d^{F-3} D^{-F+4-\beta} - \frac{k'_B}{3} \left(\frac{\mu G}{F_y} \right)^{0.5} d^{-1} D^{-\beta+2} (D - d) \right] \quad (13)$$

Figure 2 shows the dependence of modeled time evolution of floc size on the initial floc size with other parameters kept the same: $G = 7.3 \text{ s}^{-1}$, $c = 0.65 \text{ kg/m}^3$, $k'_A = 0.98$, $k'_B = 3.3 \times$

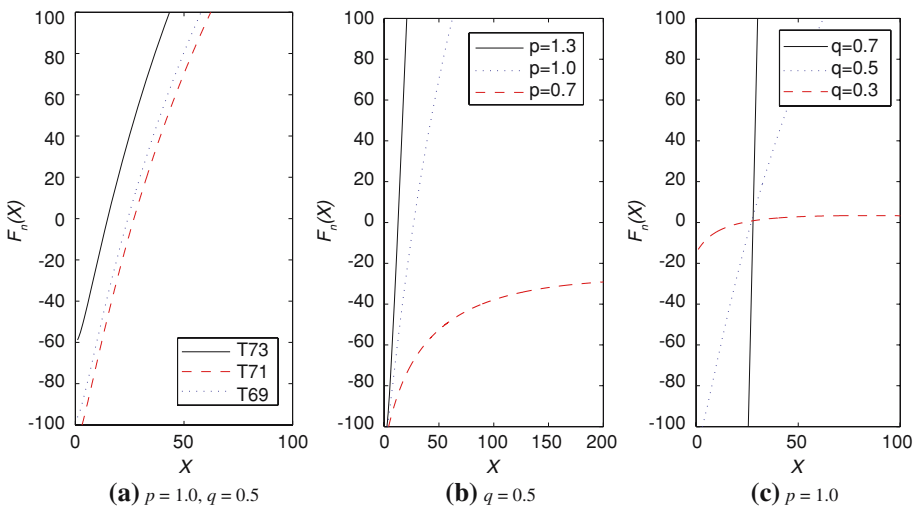


Fig. 1 Evolutions of $F_n(X)$ with X for three experiments and values of p and q . All experiments have been carried out in Delft Hydraulics. In (b) and (c), q is 0.5 and p is 1.0 and the experiment is T71 test

Table 1 Experiment values and parameters of flocculation models

Test no.	c [kg/m ³]	G [s ⁻¹]	d [μm]	F_y [N]	ρ_s [kg/m ³]	k'_A		k'_B	
						New model	Winterwerp's	New model	Winterwerp's
T71	0.65	7.3	4	10 ⁻¹⁰	2,650	0.98	0.3095	3.3 × 10 ⁻⁵	3.54 × 10 ⁻⁵
T69	1.17	28.9	4	10 ⁻¹⁰	2,650	0.98	0.3095	3.3 × 10 ⁻⁵	3.54 × 10 ⁻⁵
T73	1.21	81.7	4	10 ⁻¹⁰	2,650	0.98	0.3095	3.3 × 10 ⁻⁵	3.54 × 10 ⁻⁵

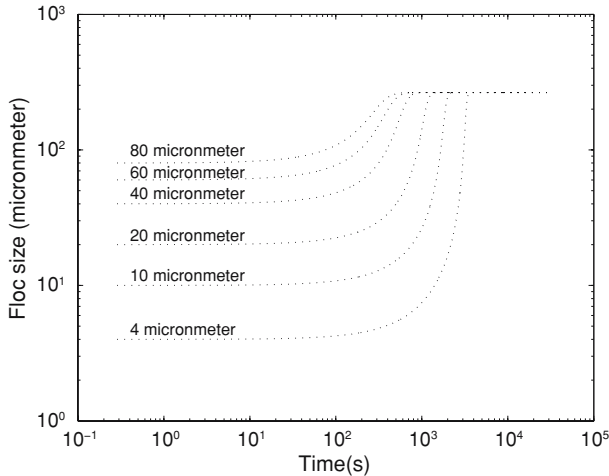


Fig. 2 Model results with different initial floc sizes (4, 10, 20, 40, 60 and 80 μm). For all cases, $G = 7.3 \text{ s}^{-1}$, $c = 0.65 \text{ kg/m}^3$, $k'_A = 0.98$, $k'_B = 3.3 \times 10^{-5}$, and $F_y = 10^{-10} \text{ N}$

10^{-5} , and $F_y = 10^{-10} \text{ N}$. It is observed that the initial floc size affects the time to reach the equilibrium state, but not on the final (equilibrium) floc size. Notice that most of the field or laboratory experiments cannot start with primary particles because it is difficult to keep all primary particles completely separated before the experiment. Model results presented here are insensitive to this uncertainty as far as the final floc size is concerned.

3 Validation of flocculation model

As shown in Eq. 13, the flocculation model depends primarily on five parameters: the floc size d and density ρ_s of the primary particle, the yield strength of flocs F_y , and empirical parameters k'_A and k'_B . In this study we follow Winterwerp [47] where d , F_y , and ρ_s are assumed to be 4 μm, $O\{10^{-10}\} \text{ N}$, and 2,650 kg/m³. Winterwerp [47] specifies these values based on experimental data and information adopted by previous literatures [25,44]. Specifically he estimates the yield strength of floc F_y , to be about $O\{10^{-10}\} \text{ N}$, but also acknowledge that for natural mud F_y may change by several order of magnitude depending on the chemical–biological properties of the floc. Finally, k'_A and k'_B are empirical coefficients that may vary with fluid/sediment properties and possibly sediment concentration (see next section). Hence, these two empirical coefficients are calibrated for each experiment.

Bouyer et al. [5] carry out experiments on floc size distribution in a mixing tank. In these experiments, a synthetic suspension of bentonite is used to mimic the behavior of particles in natural water. The concentration of bentonite is fixed at 0.03 kg/m^3 . The dissipation parameter, G , varies from 5 to 300 s^{-1} and the mean floc sizes of floc are measured for each value of G . It is assumed that the equilibrium floc size is close to the measured mean floc size of flocs. To simulate these experiments, k'_A and k'_B for the present model and Winterwerp's model are determined to be 1.82 and 1.9×10^{-6} and 1.02 and 3.8×10^{-6} by matching the model results with measured data. The results for all nine tests reported by Bouyer et al. [5] are plotted in Fig. 3, which shows the variation of the equilibrium floc size with the dissipation parameter. In this figure, the floc size predicted by the present model shows good agreement with the experimental data. The model is capable of predicting the equilibrium floc size at different levels of homogeneous turbulence.

Biggs and Lant [4] report the measured equilibrium floc sizes of activated sludge for various magnitudes of dissipation parameter. 60 ml of activated sludge is added with 1.135 liter of filtered effluent ($0.45 \text{ }\mu\text{m}$ Millipore filters) to a 1.2 l baffled batch vessel and mixed with a flat six blade impeller. Because the mass of total sludge diluted with effluent is not reported, the mass concentration is derived here from the volumetric concentration based on the assumption that the density of sludge to be $1,300 \text{ kg/m}^3$ and the density of primary particle to be $2,650 \text{ kg/m}^3$. The calculated mass concentration is 24.19 kg/m^3 and is rather concentrated. Using flat six impellers, four dissipation parameters are tested: 19.4 , 37.0 , 113 , and 346 s^{-1} . To model these experiments, we use $k'_A = 0.017$ and $k'_B = 2.4 \times 10^{-5}$ for the new model and $k'_A = 0.008$ and $k'_B = 4.4 \times 10^{-5}$ for Winterwerp's model based on best-fit of the model results with the case of $G = 19.4 \text{ s}^{-1}$. The results for all test cases are shown in Fig. 4. The floc sizes in the range of $G = 19.4$ and $G = 113.0 \text{ s}^{-1}$ are in good agreement with experimental results.

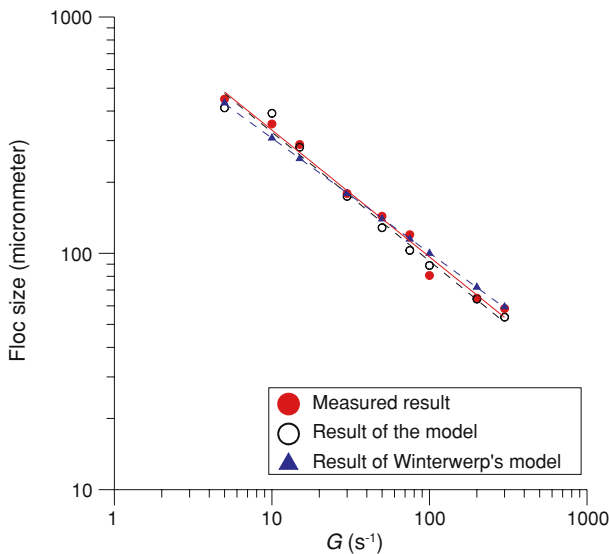
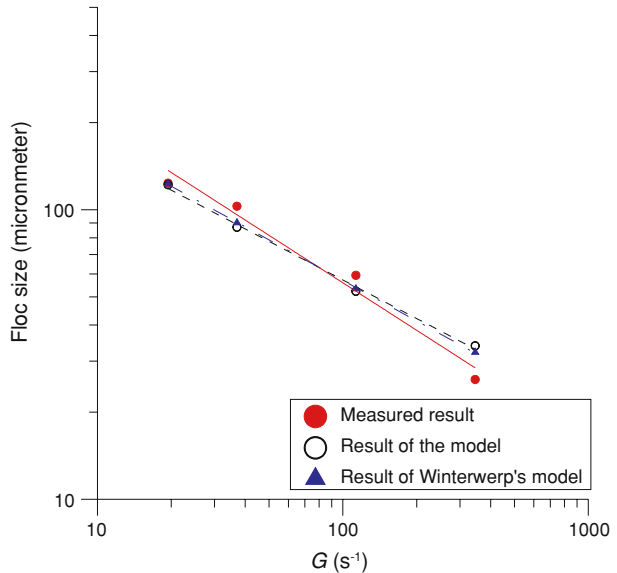


Fig. 3 Experimental results of equilibrium floc size reported by Bouyer et al. [5] and modeled results predicted by the present flocculation model and Winterwerp's model. Solid line is a regression of measured results and dotted lines are those of the flocculation models

Fig. 4 Experimental results of equilibrium floc size measured by Biggs and Lant [4] and model results by the present model and Winterwerp's model for several dissipation parameters. The solid line is a regression of measured results and the dotted lines are for results of the flocculation models



However, it is evident that the equilibrium floc sizes calculated by both the present model and Winterwerp's model show a milder slope in the log–log plot than the experimental results. Comparing the measured results between Bouyer et al. [5] and Biggs and Lant [4], it appears that the decay of equilibrium floc size (or breakup process) is enhanced when concentration is higher (see also Fig. 9).

Figure 5 presents the temporal evolution of floc size for the case of $G = 19.4 s^{-1}$. Because k'_A and k'_B are chosen to best-fit the calculated equilibrium floc size with the measured data according to this case, it allows us to evaluate the model capability on the time-dependent floc evolution. According to Biggs and Lant [4], the initial floc size is about $15 \mu m$ for this experiment. It appears that this experiment is not started with completely deflocculated primary particles because $15 \mu m$ appears to be too large for typical size of primary particles. Thus, the model calculation is conducted based on the assumption that the initial condition of cohesive sediment in the vessel is not primary particles but microflocs having larger size. Under this assumption, the initial floc size is set to be $15 \mu m$ and the primary particle size is assumed to be $4 \mu m$. The measured and modeled temporal evolutions of floc size are plotted in Figs. 5 and 6. The dotted curves of Figs. 5a and 6a represent model results using $k'_A = 0.017$, $k'_B = 2.4 \times 10^{-5}$, $p = 1.0$, and $q = 0.5$ (i.e., parameters that are identical to that shown in Fig. 4). Overall, the shapes of the floc size evolution are not predicted well by the models although the final equilibrium floc size is predicted. The measured floc evolution shows a less apparent “S-curve” shape. The floc size has a more rapid initial increase with time but shows a more gradual increase of floc size when approaching equilibrium. On the contrary, the model results predict a more gradual increase during the initial stage and approach to the equilibrium state more rapidly. In Fig. 5(a), the dashed-dot curve and dashed curve represent model results with $k'_A = 0.020$ and $k'_B = 2.84 \times 10^{-5}$ and $k'_A = 0.015$ and $k'_B = 2.13 \times 10^{-5}$, respectively. All of them use $p = 1.0$ and $q = 0.5$. The purpose of these tests is to evaluate the sensitivity of model results on k'_A but k'_B need to be changed slightly in order to match the given equilibrium floc size. It can be concluded that the shape of curve is only slightly affected by k'_A and k'_B . In order to further study the effects of p and q , three sets of p and q are

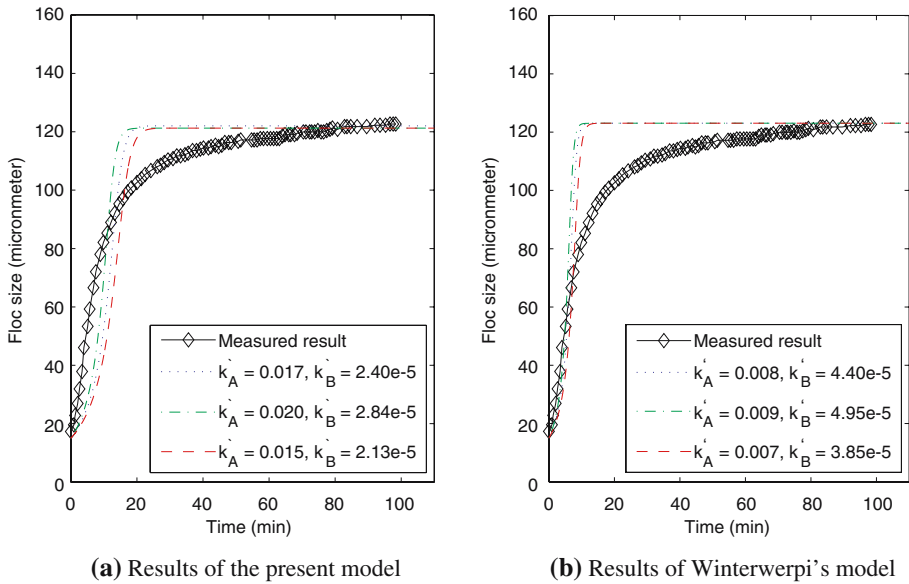


Fig. 5 Temporal evolution of floc size measured by Biggs and Lant [4] and calculated by the flocculation models for the case of $G = 19.4 \text{ s}^{-1}$. Three curves represent model results using different sets of k'_A and k'_B with fixed $p = 1.0$ and $q = 0.5$

tested (with $k'_A = 0.017$ and $k'_B = 2.4 \times 10^{-5}$) and the model results are shown in Fig. 6. The dashed-dot curve and dashed curve represent the model results with $p = 1.05$ and $q = 0.34$ and $p = 0.95$ and $q = 0.65$. Apparently, changes of p and q also do not have significant effect on the shape of the time evolution of floc size. Figure 7 represents the temporal change of fractal dimensions. As the floc sizes approach the equilibrium the values of fractal dimensions approach 2.4. Because the initial floc size is assumed to be $15 \mu\text{m}$ the initial value of fractal dimension is not 3.0 but 2.75.

Winterwerp [47] develops a flocculation model based on fixed fractal dimension and his research is one of the bases of this study. In Winterwerp [47], the model coefficients are calibrated or estimated using experimental data measured in Delft Hydraulics (see [44]). It is assumed that at $t = 0$ the initial particle size equals to the size of the primary particles, i.e., $D_0 = d = 4 \mu\text{m}$ and the maximum floc size measured equals the equilibrium value. Other values required by the flocculation model are given in Table 1 and all these values are determined from the measured results of test T73.

Figure 8 presents the results of two flocculation models. It is can be observed that flocculation model using variable fractal dimension has a slightly more smooth S-curve than that of Winterwerp [47]. Results calculated by both models are in fair agreement with experimental results in terms of the equilibrium floc size. Considering all three test cases for equilibrium floc size, model results using variable fractal dimension appear to agree with the experimental data slightly better than results of Winterwerp's model.

This is qualitatively consistent with the conclusion made by Khelifa and Hill [17] on settling velocity using variable fractal dimension.

Manning and Dyer [24] examine the relationship between floc size and dissipation parameters ($12.8\text{--}45.2 \text{ s}^{-1}$) under the condition of increasing concentration ($80\text{--}200 \text{ mg/l}$). The experiment is carried out in a laboratory flume with a nonintrusive macro-lens miniature video camera. The sediments used for the experiment have been collected from an inter-tidal

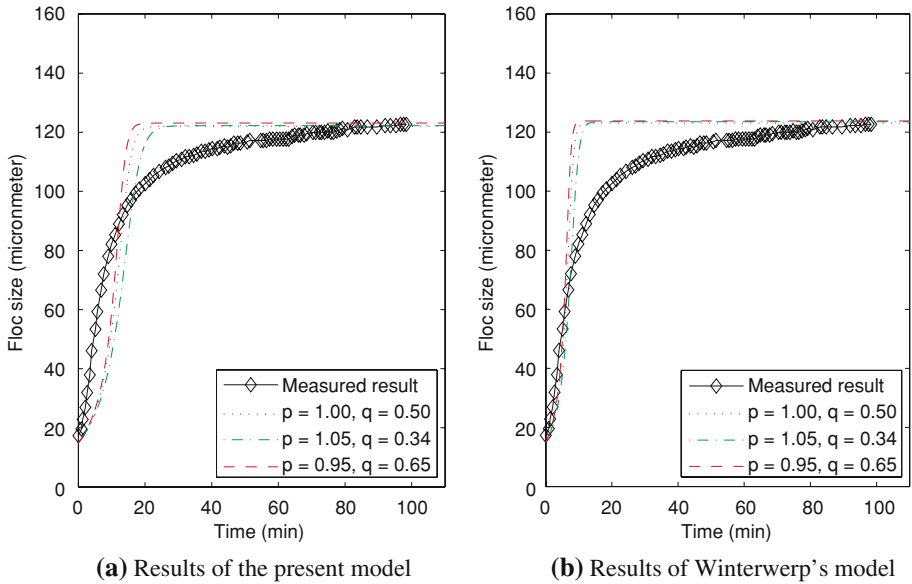
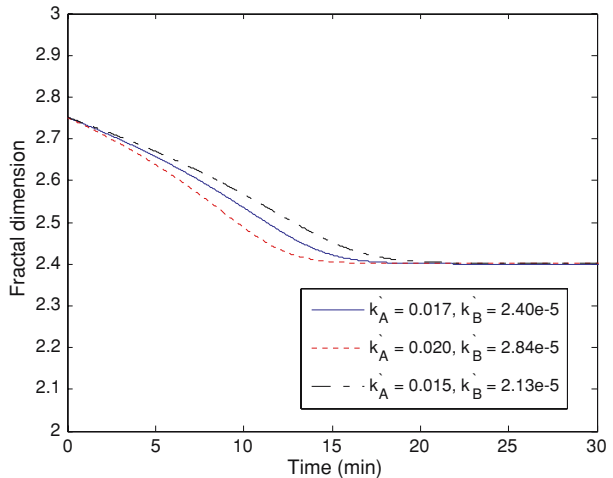


Fig. 6 Temporal evolution of floc size measured by Biggs and Lant [4] and calculated by the flocculation models for the case of $G = 19.4 \text{ s}^{-1}$. Three curves represent model results using different sets of p and q with fixed $k'_A = 0.017$ and $k'_B = 2.4 \times 10^{-5}$ for the present model and $k'_A = 0.008$ and $k'_B = 4.4 \times 10^{-5}$ for Winterwerp's model

Fig. 7 Change of the fractal dimension with time for the case of $G = 19.4 \text{ s}^{-1}$. Three lines have different sets of k'_A and k'_B with fixed $p = 1.0$ and $q = 0.5$



muflat. Figure 9 shows the results calculated by the present model using variable fractal dimension and that of Winterwerp's model. To simulate these experiments, the initial floc size is assumed to be $15 \mu\text{m}$ and k'_A and k'_B for the present model are 0.55 and 4.8×10^{-6} when $c = 120 \text{ mg/l}$ and 0.50 and 5.8×10^{-6} when $c = 160 \text{ mg/l}$. Using Winterwerp's model, empirical coefficients for k'_A and k'_B are 0.33 and 1.15×10^{-5} when $c = 120 \text{ mg/l}$ and for higher concentration $c = 160 \text{ mg/l}$ condition, k'_A and k'_B are specified as 0.30 and 1.40×10^{-5} , respectively. In the previous section, we test different types of sediments of various concentrations

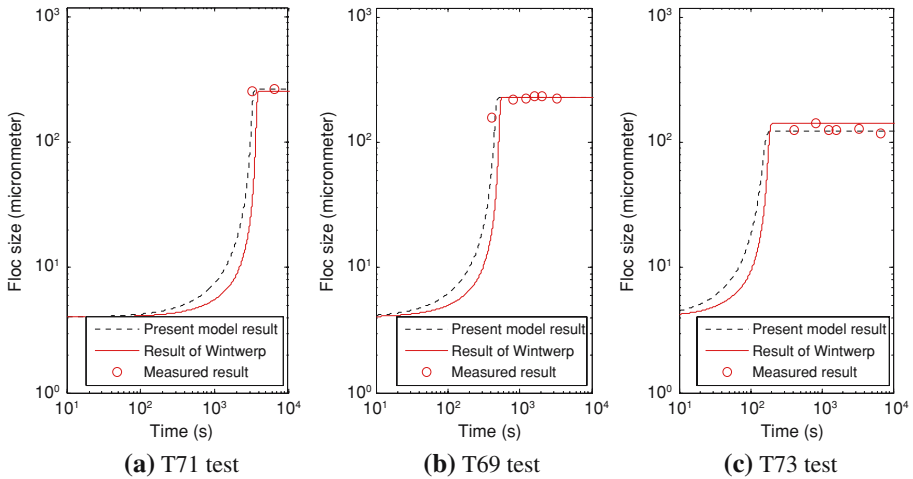


Fig. 8 Comparison of two flocculation models; Winterwerp [47] model using fixed fractal dimension and the present model using variable fractal dimension. The solid curves are the model results of Winterwerp [47], the dotted curves are the present model results, and circles are experimental data

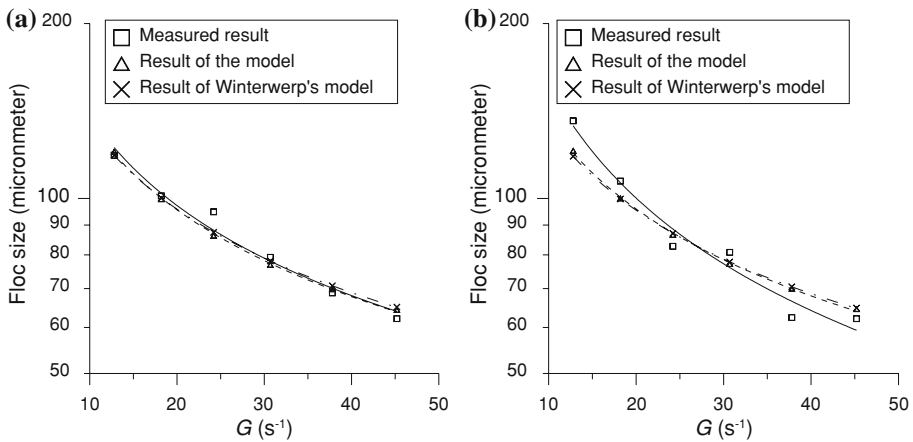


Fig. 9 Equilibrium floc sizes due to different dissipation parameters measured by Manning and Dyer [24] and the calculated results using the present model and Winterwerp’s model for mass concentration (a) 120 mg/l and (b) 160 mg/l

and the resulting empirical coefficients k'_A and k'_B are quite different. It can be concluded here that for the same sediment source considered in this case, the variation of calibrated coefficients are significantly smaller. However, it appears that these empirical coefficients may still depend on sediment concentrations despite concentration is already a variable in the aggregation term of the flocculation models. In practical applications, when the variation of sediment concentration is significant, it may be necessary to calibrate the empirical coefficients according to the magnitude of concentration.

We emphasize such a weak point of the flocculation models by further considering the decay rate of equilibrium floc size with respect to the dissipation parameter for different sediment concentrations. Flocculation models show good agreements with experimental results

when the concentration is 120 mg/l. However, when the concentration is 160 mg/l, it is evident that the regression curves of the model results for both the present model and Winterwerp's model show different slopes comparing to the experimental results. Therefore, according to measured data reported by Manning and Dyer [24], the decay rate of equilibrium floc size with respect to the dissipation parameter also depends on concentration. However, following Winterwerp's study [47], the equilibrium floc size of his model depends on the dissipation parameter G to the power of $-2/(p + 2q + F - 3)$ and the value of p and q are further chosen such that it is -0.5 . This strategy is also similarly adopted by the present model. As a result, model results can only produce more or less a single value of slope under the condition of different concentrations when the relationship between equilibrium floc sizes and dissipation parameters, G , are plotted. Future work is necessary to further study this issue. More experimental data is necessary to fully understand the decay rate of floc size with respect to the dissipation parameter for various concentrations. In addition, it is also possible to propose an empirical relation of p and q that depends on concentration.

4 Concluding remarks

This paper presents a semi-empirical model to describe flocculation process of cohesive sediment in turbulent flow. For aggregation process, the variable fractal dimension is adopted under the assumption that floc has the characteristic of self-similarity, the main concept of fractal theory. The model for breakup mechanism is based on studies of Winterwerp [47] and Kranenburg [17], which is semi-empirical and requires determination of several empirical coefficients. By a linear combination of the formulations for aggregation and breakup processes, a flocculation model which can describe the evolution of floc size with time is obtained. The values of the exponent p and q for breakup process suggested by Winterwerp [47] are shown to be also appropriate here for model based on variable fractal dimension (see Fig. 1). The capability and limitation of proposed model are validated by four experimental data sets. In terms of equilibrium floc size, model results agree reasonably well with the measured data (see Figs. 3, 4, 8 and 9(a)) provided that empirical coefficients are calibrated. This is partially because of the variation of chemical–biological properties of the cohesive sediment tested. However, through model-data comparisons with Manning and Dyer [14] (Fig. 9(b)), it becomes clear that the empirical coefficients, specifically q also depends on sediment concentration. Qualitatively, the model predicts equilibrium floc size decreases as dissipation parameter increases, suggesting that the model captures observed floc dynamics that strong turbulence has a tendency to break the floc and reduce the floc size.

As shown in Figs. 5 and 6, when comparing model results with measured time evolution of floc size by Biggs and Lant [4], the performances of the present model and Winterwerp's model are limited. Model results show a gradual increase during the initial flocculation stage and after larger aggregates are created, the floc size appears to increase too rapidly as the floc size approaching the equilibrium condition. This weak point related to time evolution of floc size cannot be improved by adjusting model coefficient such as p , q , k'_A , and k'_B (see Figs. 5 and 6). Because the flocculation model of Winterwerp [47] using fixed fractal dimension also shows similar S-shaped curve, we conclude that the existing description for floc dynamic may need to be revised for a more accurate description on the time-dependent behavior of floc size. It is likely that other term representing additional physics of floc aggregation and breakup need to be incorporated. On the other hand, if the fractal dimension is deemed to be a variable, the floc strength F_y , which is shown to be a constant under the assumption of fixed fractal dimension [19], shall also be a variable [17]. This aspect is not further investigated

in this study due to limited information on floc strength. However, it is an important future work to investigate the temporal evolution of floc size.

Although incorporating variable fractal dimension based on empirical relationship of Khelifa and Hill [17] does not improve Winterwerp's model significantly, we believe using variable fractal dimension remains to be more physically reasonable for a more extensive study of cohesive sediment transport processes, such as a unified model for sedimentation and consolidation. Jackson [16] and Thomas et al. [38] propose the model of the equivalent spherical diameter of floc considering size distribution of primary particles. Using their approaches, it is possible to develop a flocculation model of polysized particles. In this study, only monosized primary particles are considered. However, sediments in nature are the mixture of primary particles having various sizes. In order to simulate the natural phenomenon more completely, it is necessary to consider polysized primary particles.

Acknowledgements This study is supported by the U.S. Office of Naval Research (N00014-07-1-0494, N00014-07-1-0154) and National Science Foundation (CBET-0426811, OCE-0644497).

References

1. Akers RJ, Rushton AG, Stenhou JIT (1987) Floc breakage: the dynamic response of particle size distribution in a flocculated suspension to a step change in turbulent energy dissipation. *Chem Eng Sci* 42:787–798
2. Argamam Y, Kaufman WJ (1970) Turbulence and flocculation. *J Sanitary Eng ASCE* 96(SA2):223–241
3. Ayesa E, Margeli MT, Florez J, Garcia-heras JL (1991) Estimation of breakup and aggregation coefficients in flocculation by a new adjustment algorithm. *Chem Eng Sci* 46(1):39–48
4. Biggs CA, Lant PA (2000) Activated sludge flocculation: on-line determination of floc size and the effect of shear. *Water Res* 34(9):2542–2550
5. Bouyer D, Line A, Do-quang Z (2004) Experimental analysis of floc size distribution under different hydrodynamics in a mixing tank. *AIChE* 50(9):2064–2081
6. Bratby J (1980) Coagulation and flocculation with an emphasis on water and waste water treatment. Uplands Press Ltd, Croydon, England
7. Camp TR, Stein PC (1943) Velocity gradients and internal work in fluid motion. *J Boston Soc Civil Eng* 30:219–237
8. Dyer KR (1989) Sediment processes in estuaries: future research requirements. *J Geophys Res* 94(C10):14327–14339
9. Dyer KR, Manning AJ (1999) Observation of the size, settling velocity and effective density of flocs, and their fractal dimensions. *J Sea Res* 41:87–95
10. Harris CK, Traykovski PA, Geyer RW (2004) Including a near-bed turbid layer in a three-dimensional sediment transport model with application to the Eel River shelf, Northern California. In: Spaulding M (ed) Proceedings of the eighth conference on estuarine and coastal modeling. Am Soc Civ Engr, Reston, VA, pp 784–803
11. Hawley N (1982) Settling velocity distribution of natural aggregates. *J Geophys Res* 87(C12):9489–9498
12. Hill PS, Newell ARM (1995) Comparison of two models of aggregation in continental-shelf bottom boundary layers. *J Geophys Res* 100(C11):22749–22763
13. Hill PS, Voulgaris G, Trowbridge JH (2001) Controls on floc size in a continental shelf bottom boundary layer. *J Geophys Res* 106(C5):9543–9549
14. Hsu T-J, Traykovski PA, Kineke GC (2007) On modeling boundary layer and gravity-driven fluid mud transport. *J Geophys Res* 112(C04011): doi: 0.1029/2006JC003719
15. Ives KJ (1978) Rate theories. The scientific basis of flocculation. Sijthoff and Noordhoff, Alphen aan den Rijn, The Netherlands, 37–61
16. Jackson GA (1998) Using fractal scaling and two-dimensional particle size spectra to calculate coagulation rates for heterogeneous systems. *J Colloid Interface Sci* 202:20–29
17. Khelifa A, Hill PS (2006) Models for effective density and settling velocity of flocs. *J Hydraul Res* 44(3):390–401

18. Kramer TA, Clark MM (1999) Incorporation of aggregate breakup in the simulation of orthokinetic coagulation. *J Colloid Interface Sci* 216:116–126
19. Kranenburg C (1994) The fractal structure of cohesive sediment aggregates. *Estuarine Coastal Shelf Sci* 39:451–460
20. Leentvaar J, Rebhun M (1983) Strength of ferric hydroxide flocs. *Water Res* 17:895–902
21. Levich VG (1962) *Physicochemical hydrodynamics*. Prentice Hall
22. Lick W, Huang H, Jepsen R (1993) Flocculation of fine-grained sediments due to differential settling. *J Geophys Res* 98(C6):10279–10288
23. Lick W, Lick J (1988) Aggregation and disaggregation of fine-grained lake sediments. *J Great Lakes Res* 14:514–523
24. Manning AJ, Dyer KR (1999) A laboratory examination of flocc characteristics with regard to turbulent shearing. *Mar Geol* 160:147–170
25. Matsuo T, Unno H (1981) Forces acting on flocc and strength of flocc. *J Env Engr Div ASCE* 107(EE3):527–545
26. McAnally WH, Mehta AJ (2000) Aggregation rate of fine sediment. *J Hydraul Engr* 126:883–892
27. McCave IN (1984) Size spectra and aggregation of suspended particles in the deep ocean. *Deep Sea Res* 31(4):329–352
28. Meakin P (1988) Fractal aggregates. *Adv Colloid Interface Sci* 28:249–331
29. Mehta AJ (1987) On estuarine cohesive sediment suspension behavior. *J Geophys Res* 94(C10):14303–14314
30. Merckelbach LM, Kranenburg C (2004) Determining effective stress and permeability equations for soft mud from simple laboratory experiments. *Geotechnique* 54(9):581–591
31. Merckelbach LM, Kranenburg C, Winterwerp JC (2002) Strength modeling of consolidating mud beds. In: Winterwerp JC, Kranenburg C (eds) *Fine sediment dynamics in the marine environment*. Elsevier, p 359
32. Migniot C (1968) A study of the physical properties of various forms of very fine sediments and their behaviour under hydrodynamic action. *Comunication présentée au Comité Technique de la Société Hydrotechnique de France, La Houille Blanche* 23(7):591–620
33. O'Melia CR (1980) Aquasols: the behaviour of small particles in aquatic systems. *Env Sci Technol* 14(9):1052–1060
34. Parker DS, Kaufman WJ, Jenkins D (1972) Flocc breakup in turbulent flocculation processes. *J Sanitary Engr Div* 98(SA1):79–97
35. Smoluchowski M (1917) Versuch einer Mathematischen Theorie der Koagulationskinetik Kolloidlösungen. *Zeitschrift für Physikalische Chemie* 92:129–168
36. Stolzenbach KD, Elimelech M (1994) The effect of density on collisions between sinking particles: implications for particle aggregation in the ocean. *J Deep Sea Res* 13:409–419
37. Tambo N, Hozumi H (1979) Physical characteristics of flocs-II: Strength of flocc. *Water Res* 13:421–427
38. Thomas DN, Judd SJ, Fawcett N (1999) Flocculation modeling: A review. *Water Res* 33(7):1579–1592
39. Toorman EA (1999) Sedimentation and self-weight consolidation: constitutive equations and numerical modeling. *Geotechnique* 49(6):709–726
40. Traykovski P, Geyer WR, Irish JD, Lynch JF (2000) The role of wave-induced fluid mud flows for cross-shelf transport on the Eel River continental shelf. *Continental Shelf Res* 20:2113–2140
41. Tsai CH, Hwang SC (1995) Flocculation of sediment from the Tanshui River estuary. *Mar Freshwater Res* 46:383–392
42. Tsai CH, Iacobellis HS, Lick W (1987) Flocculation of fine-grained sediments due to a uniform shear stress. *J Great Lakes Res* 13(2):135–146
43. Van Der Ham R, Winterwerp JC (2001) Turbulent exchange of fine sediments in a tidal channel in the Ems/Dollard estuary: Part II. Analysis with a 1DV numerical model. *Continental Shelf Res* 21:1629–1647
44. van Leussen W (1994) *Estuarine macroflocs and their role in fine-grained sediment transport*. University of Utrecht, Dissertation
45. Vicsek T (1992) *Fractal growth phenomena*. McGraw-Hill, New York
46. Warner JC, Sherwood CR, Signell RP, Harris CK, Arango HG (2007) Development of a three-dimensional, regional, coupled wave, current and sediment-transport model. *Computers Geosci*, accepted
47. Winterwerp JC (1998) A simple model for turbulence induced flocculation of cohesive sediment. *J Hydraul Res* 36(3):309–326
48. Winterwerp JC (2002) On the flocculation and settling velocity of estuarine mud. *Continental Shelf Res* 22:1339–1360

49. Winterwerp JC, Manning AJ, Martens C, Mulder T, Vanlede J (2006) A heuristic formula for turbulence-induced flocculation of cohesive sediment. *Estuarine Coastal Shelf Sci* 68:195–207
50. Winterwerp JC, Van Kesteren WGM (2004) Introduction to the physics of cohesive sediments in the marine environment. In: *Developments in sedimentology*, vol 56. Elsevier, New York